Supporting Information for:

The consequences of daily cyclic hypoxia on the European grass shrimp Palaemon varians: from short-term responses to long-term effects

L. Peruzza; M. Gerdol; A. Oliphant; D. Wilcockson; A. Pallavicini; L. Hawkins; S. Thatje; C. Hauton

Materials and Methods:

Sampling site, animal collection and maintenance:

The population of *Palaemon varians* used in experimental work originates from the salt marsh of Lymington in southern Hampshire (UK, location: 50°44'19.8" N and 50°44'22.2" W). Since 1973, these salt marshes have been part of the "Lymington-Keyhaven nature reserve" and play a key role as nursery habitats for bird, fish and invertebrates. Water pO_2 inside the channel was measured by building a custom oxygen-logger, consisting of an Anderaa Oxygen Optode model 3835 (Xylem, USA) fitted with an internal temperature sensor and connected with a cable to an r-p-r space logger S10 (Richard Paul Russell Ltd, Southampton, UK) and a 12V battery. Logger and battery were housed in a waterproof box. In order to quantify some of the daily pO_2 variation that can occur in the ditch pO_2 data was continuously measured in three discrete weeks (August 4th – 11th 2016; February 16th – 23rd 2017; May 14th – 22nd 2017). For the entire duration of each sampling week, the oxygen optode measured water temperature (˚C) and air saturation (%) every 10 minutes. The

optode was fixed to a metal stake and placed in the centre of the channel and adjacent to the bottom of the channel (approximately 5 – 10 cm from the bottom of the channel).

Adult *Palaemon varians* used for all experiments were net-caught from this site on different occasions (see Supplementary Table 2 for details showing the field sampling date in which animals used in each experiment were collected). Within one hour from collection, adult *P. varians* were recovered to the National Oceanography Centre Southampton inside 10L water buckets filled with water from the channel. Adults were kept in 150L aquaria with UV-sterilised and filtered seawater (salinity 33 PSU), filtration systems and air stones, and slowly acclimated to the experimental temperature of 22˚C (+1˚C/day). Animals were fed three times/week with commercial shrimp granules (shrimp naturals – Sera, Germany) and water was changed once per week. One week before the experiment, animals were haphazardly distributed into the experimental tanks.

General experimental protocol:

Hypoxia was defined as pO_2 < critical oxygen pressure (p_{crit}). In order to calculate p_{crit}, a closed respirometer with a total sea water volume of 55mL was placed inside a water bath with seawater at 33 PSU at a constant temperature of 22 ˚C. P_{crit} was determined at 22 ˚C as this temperature is frequently measured in the marsh during summer (from June to September) at night (from 2000 to 0800 BST, Supplementary Fig. 1A). A Fibox 3 optical oxygen meter (PreSens Precision Sensing GmbH, Germany) equipped with an O_2 sensor spot was used to monitor pO_2 in the respirometer. The sensor spot was fixed on the inner surface of the respirometer and pO_2 could therefore be continuously measured in a non-

47 invasive and non-destructive manner from outside. The instrument was calibrated daily with
48 100% O_2 saturated seawater and 0% O_2 saturated seawater (Oliphant et al., 2011). Every
49 evening one shrimp was placed inside the respirometer to acclimate overnight. The
50 following day the respirometer was sealed and pO_2 was measured every 30 seconds. The
51 experiment ended: *i)* when pO_2 reached 0 kPa or *ii)* when pO_2 was near 0 kPa but was no
52 longer decreasing. At the end of each experiment the animal was carefully blotted on paper
53 and its wet weight was taken with an analytical balance (Denver Instrument si-234 Colorado
54 - USA, weight ± 0.0001g). Each mean pO_2 value (calculated over an interval time of three
55 minutes) was converted to oxygen concentration (µmol L^{-1}) under the temperature and
56 salinity conditions used in the experiment according to Benson and Krause (1984). Oxgen
57 consumption rate MO_2 (µmol O_2 g^{-1} min^{-1}, Ern, Huong, Nguyen, Wang, and Bayley (2013))
58 was calculated from the measured pO_2 values according to the relation (Oliphant & Thatje,
59 2014):
60
61 $$MO_2 = [([O_2]_{initial} - [O_2]_n) / t_n] * V / WW$$
62
63 Where: $[O_2]$ is the oxygen concentration in the water (in µmol/l); t_n is the time (min); V is the
64 volume of the chamber (L); WW is the wet body mass of the animal (g).
65
66 MO_2 was plotted against pO_2 and fitted with a curve using Prism 6 (GraphPad Software, San
67 Diego, CA) after comparing different non-linear models (as suggested by Marshall, Bode,
68 and White (2013)). Among all the models, the logarithmic model gave the best fit in terms
69 of R^2 values and was therefore chosen. P_{crit} was then calculated according to Mueller et al
70 (2011), by finding the highest vertical distance between the fitting curve (i.e. the logarithmic

model) and the straight line (representing hypothetical perfect conformity, according to Herreid (1980)) passing through the curve values at the initial and final pO_2 values recorded during the experiments. P_{crit} was determined individually for every animal used (Supplementary Table 1) and then a mean value was calculated (n=10).

To perform all subsequent experimental work, two flow-through experimental systems were built (one system for cyclic hypoxic treatment, one for normoxic treatment). All experimental work in these systems was conducted in filtered seawater at 33 PSU and 22 ˚C with a day-night cycle of 12:12 h, except for the reproductive experiment where a 16:8 day:night cycle was used. Each flow-through system comprised three 1L flasks, each one connected to a 12L aquarium (in which animals were held). Before recirculation back into the system, outflow water was subject to mechanical and chemical filtration in a 60L sump. Hypoxia was achieved by independently bubbling N_2 in each of the three 1L flasks and water pO_2 was continuously measured and logged with Microx TX 3 (PreSens) sensors. Water and N_2 flow-rate were adjusted in order to obtain $pO_2<p_{crit}$. Animals were subjected hypoxic conditions (i.e. pO_2 < 4.5 kPa) for 7 hours (from 0230 to 0930 hrs) and they were kept in normoxic conditions (by bubbling air into the system) for the rest of the day (Supplementary Fig. 1B). In the normoxic flow-through system air was bubbled to prevent the development of hypoxic conditions. For each experiment, the duration (in terms of days) of the exposure and the mean±SD pO_2 level recorded during hypoxic periods in each tank is reported in Supplementary Table 2.

In experiments investigating inter-moult duration, changes in the expression of cuticular genes throughout an entire moult cycle and gill histology, a synchronous population (composed of similar-size animals that had all moulted within 12 hours) was

used, whereas no animal selection was made according to the stage of the moult cycle during experiments involving RNA-seq, growth, feeding, excretion and reproduction.

Transcriptome response to hypoxia

In this experiment, no animal selection was made according to the stage of the moult cycle, therefore animals were not necessarily in the same moult stage. The experiment was performed to identify changes in gene expression after seven days of cyclic hypoxic exposure. Animals (n=8 per treatment) were randomly sampled at 1030 hrs after seven days of exposure to experimental conditions (cyclic hypoxia or normoxia) and the cephalothorax snap frozen in liquid N_2. Total RNA was extracted from whole cephalothorax using a TRI-Reagent™ (Sigma Aldrich) protocol according to the manufacturer's recommendations. RNA concentration was determined using a NanoDrop™ spectrophotometer (Thermo Fisher Scientific). Experion™ (Bio-Rad, UK) electrophoresis was used to assess RNA integrity and only samples with RQI>9 were used. For both treatments (hypoxia and normoxia), RNA from samples was pooled (i.e. two pools, hypoxia and normoxia, where created, each comprising an equal amount of RNA from each sample). Library preparation followed Illumina TruSeq RNA Library Preparation Kit v2 (Illumina, California) according to the manufacturer's protocol. Paired-end 115bp reads were sequenced on a single lane of an Illumina HiSeq 2500 platform at the IBERS Translational Genomics facility, Aberystwyth University. Raw sequencing data were imported into the CLC Genomic Workbench v.8.5 (CLC Bio, Aarhus, Denmark) environment, where reads were trimmed to remove residual sequencing adapters, low quality bases and ambiguous nucleotides. The reference transcriptome for the subsequent gene expression study was

obtained with the *de novo* assembly tool, using automatically set *bubble size* and *word size* parameters. The assembly was further refined by removing contigs displaying a very low sequencing coverage (<5 X), as these could be the results of excessive fragmentation of longer transcripts, mis-assembly or contamination from exogenous RNAs, altogether contributing to background noise, as suggested by Carniel et al. (2016). The quality of the assembled transcriptome was tested, in terms of completeness and integrity, with BUSCO v.3 (Simao, Waterhouse, Ioannidis, Kriventseva, & Zdobnov, 2015), using the core set of metazoan single copy orthologous genes as a reference.

The RNA-seq analysis tool of the CLC Genomics Workbench was then used to calculate gene expression levels in the two samples. Trimmed reads were first mapped to the reference transcriptome with 0.75 and 0.98 as *length fraction* and *similarity fraction* parameters. To allow comparability of expression values between the two samples, read counts were normalized by totals, assuming a virtual number of 1 million reads per sample.

The reference transcriptome was annotated with the Trinotate pipeline (Grabherr et al., 2011). Briefly, the protein translation of each contig were predicted with TransDecoder, assuming a minimum ORF length of 100 codons. Contigs and virtually translated proteins were BLASTed against the UniprotKB database to detect significant homology with known sequences (based on an-e-value threshold of $1x10^{-5}$), and corresponding Gene Ontology annotations were subsequently extracted. At the same time, amino acidic sequences were screened with InteroProScan (Quevillon et al., 2005) to annotate conserved protein domains contained.

Statistically significant gene expression changes, both in terms of up-regulation and down-regulation between the hypoxia and control samples, were detected by the use of a

Kal's Z-test (Kal et al., 1999). Contigs were considered as differentially regulated for proportion Fold Change values >2 or <-2, supported by FDR-corrected p-values ≤0.05. The subsets of up-regulated and down-regulated genes were separately subjected to hypergeometric tests (Falcon & Gentleman, 2007) on Gene Ontology and Pfam annotations, to detect significantly over-represented terms which might be indicative of alterations of biological pathways underpinning the observed gene expression changes.

The expression of some up-regulated genes was further confirmed by means of quantitative-PCR analysis (following protocols described below in "Gene expression pattern" section). Statistical significance was identified at $P<0.05$ as determined by t-test after testing for normality (Shapiro test) and homogeneity of variances (Bartlett test) using R statistical software (R Core Team (2014)).

Gene expression of cuticular genes during moult cycle

To investigate changes in gene expression during the moult cycle, shrimps from a synchronous population were, within 12 hours from ecdysis, randomly allocated to the hypoxic (n=54) or normoxic (n=54) treatment and exposed to experimental conditions for up to 16 days. Every other day, from the day of ecdysis (day 0) up to 16 days after this event (day 16), cephalothoraxes from animals (n=6 per treatment) were collected and flash frozen (between 1000 and 1030 hrs) in liquid N_2. Total RNA was extracted from whole cephalothorax and concentration and integrity assessed as above.

A volume containing 1.5 µg of total RNA was treated with Promega RQ1 RNase-free DNase (Promega Corporation, Hants, UK) according to the manufacturer's protocol. Total

RNA (0.68µg) was reverse transcribed in a 20µl reaction using Superscript III reverse transcriptase (Invitrogen, UK) and oligo$(dT)_{20}$ primers.

All qPCR reactions were performed on a LightCycler 96 (Roche, Switzerland). Each 25 µl reaction contained 12.5 µl of Precision Plus 2× qPCR Master mix (Primer-Design, UK) with SYBR green, and 1 µl of template cDNA. qPCR conditions were: 1 cycle of 95°C for 5 min, 40 cycles of [95°C 10 s, 60°C 1 min], followed by 72˚C for 45 sec. Each reaction was run in duplicate (technical replicate) with the addition of three inter-run calibrators in each 96-plate. After each run a melt curve analysis was performed in order to demonstrate the specificity of the qPCR products.

Primer-sets used are reported in Table 1. All primer-sets tested generated a single and discrete peak by melt curve analysis. As specified by the MIQE guidelines (Bustin, 2010), all primer-sets had an efficiency of between 90-105% and linearity greater than r^2=0.98 across four 10-fold serial dilutions.

Elongation factor 1-alpha gene (*eef1A*) and ribosomal protein L8 gene (*rpl8*) were used as reference genes in all experiments after assessing their stability as housekeeping genes with qBase+ software (Biogazelle, UK). Their stability (i.e. geNorm M value) was lower than 0.5 and their coefficient of variation was lower than 0.2. Indications from the transcriptome (on up-regulated contigs in relation to hypoxia) were used to select three genes of interest for qPCR analysis: post-moult protein - *PMP* (Roer, Abehsera, & Sagi, 2015), calcification-associated peptide - *CaAP* (Inoue, Ohira, Ozaki, & Nagasawa, 2004), and peptide DD5 - *DD5* (Ikeya, Persson, Kono, & Watanabe, 2001). All three marker genes were selected because they are highly expressed during the post-moult phase of the moult cycle and contribute to the deposition and calcification of the newly formed exoskeleton (Ikeya et

al., 2001; Inoue et al., 2004; Roer et al., 2015)). Their expression throughout an entire moult cycle was then characterized using qPCR.

After testing for stability using with geNorm analysis using qBase+ software, the geometric mean of the two reference genes was used to normalise gene of interest expression. Calibrated, normalised relative quantities (CNRQs) were calculated using qBase+ software.

To test whether the overall pattern of gene expression of target genes was different between treatments, a general additive model (GAM) in R was run for each gene, using package 'mgcv' (Wood, 2006). For each gene, one GAM model fitting separately the overall gene expression pattern in hypoxia and normoxia (i.e. Model 2) was compared with a simpler GAM model fitting together all data points (independently from the treatment, Model 1). Model 1 was generated to account for the natural variability of the species in relation to the length of the moult cycle, while Model 2 was generated to account for differences in the patterns caused by the treatment. For each gene, "Akaike's Information Criterion" – AIC – values (Sakamoto, Ishiguro, & Kitagawa, 1986) between models (the model with treatments and the model without) were compared. A difference in the 2-9 range between AIC values of models was considered significant and the model with lower AIC was chosen (Burnham, Anderson, & Huyvaert, 2011).

Changes to phenotype in *Palaemon varians*: gill modification in response to cyclic hypoxia

Shrimps from a synchronous population were, within 12 hours from ecdysis, randomly allocated to the hypoxic (n=5) or normoxic (n=5) treatment and exposed to

experimental conditions for 18 days to make sure they completed one entire moult cycle in experimental conditions.

After 18 days, wet weight and total length of each individual was recorded. Animals were then chilled on ice and the cephalothorax dissected with a single transverse cut between thorax and abdomen. The cephalothorax was fixed in Bouin's solution (BDH Gurr) for 24 hours at room temperature. Samples were dehydrated in a graded ethanol series (50%, 70%, 90%, 100% and 100% anhydrous ethanol) for 24 hours at each stage, cleared in xylene and xylene-paraffin for eight and twelve hours respectively, and then embedded in paraffin wax.

Longitudinal, 5-µm sections of gill were sectioned from each sample using a rotary microtome (Leitz Wetzler, model 1212), mounted on glass slides and stained with haematoxylin and eosin (Cellpath Ltd). All microscope analysis was carried out using an Olympus BH-2-RFCA research microscope fitted with a Nikon Coolpix E4500 microscope camera. For each sample, longitudinal sections of the body produced transverse sections of gill-plates (or lamellae (Sun et al., 2015)). Lamellae from the sixth gill of each animal were analysed using ImageJ software (Schneider, Rasband, & Eliceiri, 2012). To avoid bias in picture analysis, a single-blind procedure was followed and the observer ignored which pictures belonged to which treatment. Each lamella was fitted with the "fit ellipse" function in ImageJ that returned the best-fitting ellipse for each lamella. Together with the best-fitting ellipse, the program returned major ellipse axis (lamellar length) and minor ellipse axis (lamellar thickness) of the fitting ellipse (Supplementary Figure 1). Lamellar perimeter (lamellar surface area) was then calculated with the formula:

$$2*\pi* \sqrt{[(MA/2)^2 + (ma/2)^2]}/2$$

where “MA” is the major axis and “ma” the minor axis. Lamellar density was calculated measuring the space between 15 consecutive lamellae, divided by the number of lamellae. For each parameter (i.e. lamellar width, length, perimeter and density), mean values throughout the thickness of the gill were calculated and then normalized using animal’s wet weight (mg) to account for differences in body weight among animals. Statistical difference between controls and hypoxic gills was assessed using t-test, with a cut-off p-value <0.05.

Changes in body size:

Prior to the experiment, in order to reduce variability in size and weight, a population of experimental animals with a wet weight range between 200mg and 300mg (±0.5mg) was selected (as they represent the most frequent size in Lymington, personal observation). No selection criteria for moult stage was applied; hence animals were not necessarily in the same moult stage (i.e. all in inter-moult or pre-moult). The random animal allocation to the treatment (hypoxia or normoxia) and to the experimental tanks (6 cyclic hypoxic and 6 normoxic tanks, n=17 animals per tank) was achieved by using a custom Python script (Python Software Foundation, https://www.python.org) to generate random numbers. At the beginning of the experiment, no statistical difference in weight was found between the hypoxic and normoxic group following random allocation of the animals (unpaired t-test, t=0.363, df=202, p=0.72). To investigate variations in wet weight, animals were kept in cyclic hypoxia for 28 days and changes in wet weight were compared with a control population kept in normoxia for 28 days.

During the experiment, animals were fed three-times per week using commercial shrimp granules (shrimp naturals – Sera, Germany) at a ratio of one granule per shrimp (~

259 4.8% of animal's mean wet weight). At the beginning of the experiment (day 0) and every
260 seven days to 28 days, animals were weighed using an analytical microbalance (Denver
261 Instrument si-234 Colorado - USA, weight ± 0.1mg). Animals were starved for two days
262 before their wet weight was determined in order to avoid bias due to ingested food.
263 The absence of systematic differences between the twelve experimental replicates
264 (i.e. tanks) was tested on weight data collected at day 28 by using a mixed model nested
265 Anova with the factor "tank" nested within the factor "treatment" (i.e. hypoxia and
266 normoxia). This assessment was necessary to validate the accuracy of the experimental
267 replicates. Initially weight data were tested for normal distribution with Shapiro-test.
268 Because normal distribution criteria were not met, weight data were transformed, dividing
269 the final weight (i.e. weight at day 28) of each shrimp ($fw_{tank"a"}$) by the mean initial weight
270 of the tank in which the shrimp was kept (i.e. tank "a" mean weight at day 0: $MW_{tank"a"}$),
271 using this formula:
272 Transformed data = $(fw_{tank"a"} / MW_{tank"a"})$
273 Following transformation, mixed model nested Anova was performed. The presence of
274 systematic differences between experimental replicates (i.e. the factor "tank" nested within
275 "treatment") was identified at p-value <0.05.
276 To test whether the slope of the weight-time relationship changed between
277 treatments, a linear regression model fitting separately data from hypoxia and from
278 normoxia (Model 2) was compared with a simpler model fitting all data points, regardless of
279 the treatment (Model 1). The same intercept was used for both models, since random
280 animal allocation was performed prior to the experiment. An extra sum-of-squares F test
281 from the software GraphPad Prism v7.0 was used to compare the models, and Model 1 was
282 preferred over Model 2 unless the outcome of the F test was significant ($p < 0.05$).

Feeding and excretion:

Adult *P. varians* were maintained in cyclic hypoxia or normoxia for 21 days. Feeding and excretion were quantified after 1 and 21 days of exposure on animals individually held during the tests.

In order to quantify feed ingestion, adults from both treatments (n=11 animals/treatment) were individually placed in retention chambers (one adult per chamber) made with 10cm Petri dish bottoms and 15cm high mesh (0.5 mm radius) collars, in accordance with Brouwer et al. (2007). Adults from the cyclic hypoxic group were fed while experiencing hypoxic conditions (i.e. $pO_2 < 4.5$ kPa), while adults from the normoxic group were fed in normoxic conditions. Each adult was fed (~4.5% its wet weight) with commercial pellet (shrimp naturals – Sera, Germany) and, after 150 minutes, uneaten feed was carefully collected and dried in an oven at 70 ˚C. Feed dry weight was measured with an analytical microbalance (Denver Instrument si-234 Colorado - USA, weight ± 0.1mg). Feed ingestion was calculated as follows:

$$I = [(DW_{granule} - DW_{uneaten\_feed\_a}) / DW_{granule}] / BM_a$$

$DW_{granule}$ is the mean dry weight (mg) of a commercial granule soaked in water at 22 ˚C for 150 minutes and dried in oven. $DW_{uneaten\_feed\_a}$ is the uneaten feed from animal “a”, BM_a is the wet weight (g) of animal “a”.

In order to quantify ammonium excretion, adults (n=14-18 adults/treatment) were individually placed in glass bottles with 200 mL of artificial sea-water at the same

temperature, salinity and pO_2 of their respective experimental aquaria (i.e. water $pO_2 < 4.5$ kPa for the hypoxic group, while water $pO_2 = 21$ kPa for the normoxic group). After 210 minutes, water samples were collected and ammonium ions were measured with a Hach method 8155 "Ammonia Salicylate Method" (Hach, Colorado USA) following the manufacturer's protocol, in accordance with Fass, Ganaye, Urbain, Manem, and Block (1994); Qing et al. (2016).

Two-way ANOVA with treatment and time as factors was used to assess differences in feed ingestion and ammonium excretion, followed by Tukey's multiple comparisons test. For all analysis, statistical significance was identified at $p<0.05$.

Reproduction:

Adult *P. varians* were collected in February 2016. For breeding, *P. varians* were sexed using a stereomicroscope and males were identified by the presence of the appendix masculine on the second pleopod pair, which is absent in females (Oliphant, 2013). Females containing white ovaries in primary vitellogenesis (Bouchon, 1991a) were used during the experiment. Breeding and spawning in *P. varians* are induced by long day length (Bouchon, 1991b). Hence day length was increased by two hours per day until a 18:6 light:dark cycle was achieved. Reproductive pairs of ditch shrimps (in total 12 pairs in hypoxia and 10 pairs in normoxia) were housed in retention chambers made with 10cm Petri dish bottoms and 15cm high collars of mesh (Brouwer et al., 2007). In each experimental tank, up to six retention chambers were accommodated in vertical position (i.e. with the Petri dish at the bottom of the tank), in order to maximise water flow throughout the chamber.

In order to quantify the impact of cyclic hypoxia on reproduction, reproductive pairs were kept in cyclic hypoxia for 40 days and reproductive success (in terms of ratio between gravid and non-gravid females), relative fecundity and egg dry weight were compared with control pairs kept in normoxia. Pairs were checked daily for egg production, and females were determined gravid when the presence of pleopodal eggs for two consecutive days was confirmed (Brouwer et al., 2007). All eggs were then gently removed using a pair of tweezers and counted and the total length and wet weight of each female was recorded. Relative fecundity was calculated as the number of pleopodal eggs divided by the wet weight of the female. Egg dry weight was measured after samples had been freeze-dried for 24 hours using a Thermo Scientific Heto PowerDry LL33000 freeze dryer. Samples were weighed for dry weight using a Sartorius microbalance ME5. Given the fact that heavier females are able to produce heavier eggs, egg dry weights were normalized using female wet weight.

A Chi-square test was used to test alteration in the reproductive success (number of reproductive couples versus non-reproductive couples). To assess statistical differences in relative fecundity and dry weight among treatments, student t-tests was used (after testing for normality - Shapiro test - and Homogeneity of Variances - Bartlett test) using statistical software R (Team, 2014). For all analysis, statistical significance was identified at $p<0.05$.

Results:

Animal	P_{crit} (kPa)	R^2	Sex	Wet Weight (mg)
1	5.5	0.95	-	282.2
2	3.5	0.96	Female (with eggs)	266.1
3	4.0	0.86	Female	289.4
4	4.5	0.82	Male	229.5
5	4.5	0.8	Male	116.7
6	4.5	0.79	Female	304.2
7	3.5	0.79	Male	160.8
8	4.5	0.65	Male	110.4
9	4.5	0.68	Male	227.8
10	5.0	0.61	Female (with eggs)	371.6

Table S1: P_{crit} calculated for 10 experimental animals at 22˚C. R^2 represents the goodness-of-fit for the logarithm model fitting MO_2-pO_2 data. Wet weight of each animal is reported.

Experiment:	Duration (days)	Tank 1	Tank 2	Tank 3	Animal field collection date:
Transcriptome response	7	2.9 ±0.7	3.0 ±0.6	2.1 ±0.6	Jun-2015
Inter-moult duration	up to 16	2.1 ±0.5	2.1 ±0.6	2.8 ±0.7	Feb-2016
Gene expression during moult cycle	up to 16	3.5 ±0.4	2.7 ±0.5	2.5 ±1.0	Feb-2017
Gill modifications	18	3.5 ±0.4	2.7 ±0.5	2.5 ±1.0	Feb-2017
Growth	28	2.9 ±0.9	3.1 ±0.6	3.0 ±0.9	Jun-2016
Feeding/Excretion	21	2.7 ±0.4	2.8 ±0.3	2.9 ±0.2	Mar-2017
Reproduction	up to 40	2.8 ±0.8	2.8 ±0.9	2.9 ±1.1	Feb-2016

Table S2: Mean pO_2 levels (kPa ±SD) during hypoxic trials for each replicate tank for each experiment. For every experiment, it is reported the sampling date in which animals (used for a specific experiment) were collected from the field (last column).

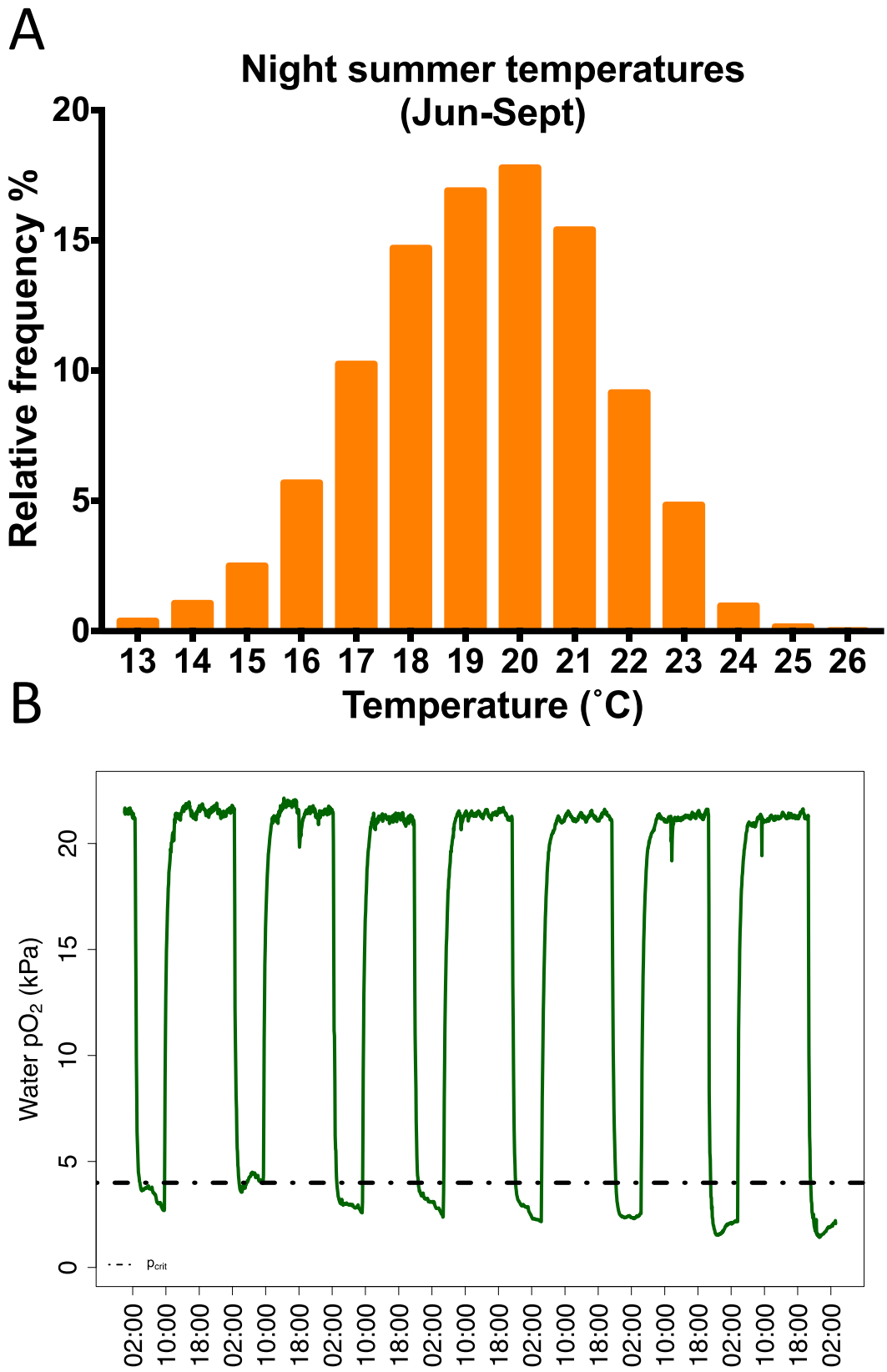

363

364 Figure S1: **A)** Frequency histogram of temperatures recorded in Lymington salt marsh

365 between 2000 hrs and 0800 hrs (BST) in summer (i.e. June – September) from 2014 to 2016.

B) Schematic representation of daily cyclic hypoxic regime (red line) during all laboratory experiments. At 22˚C, 21 kPa ~ 100% air-saturation. Dash-dotted black line represents the critical pO_2 (4.55 kPa, ~21.6% air-saturation) for the studied population at 22˚C.

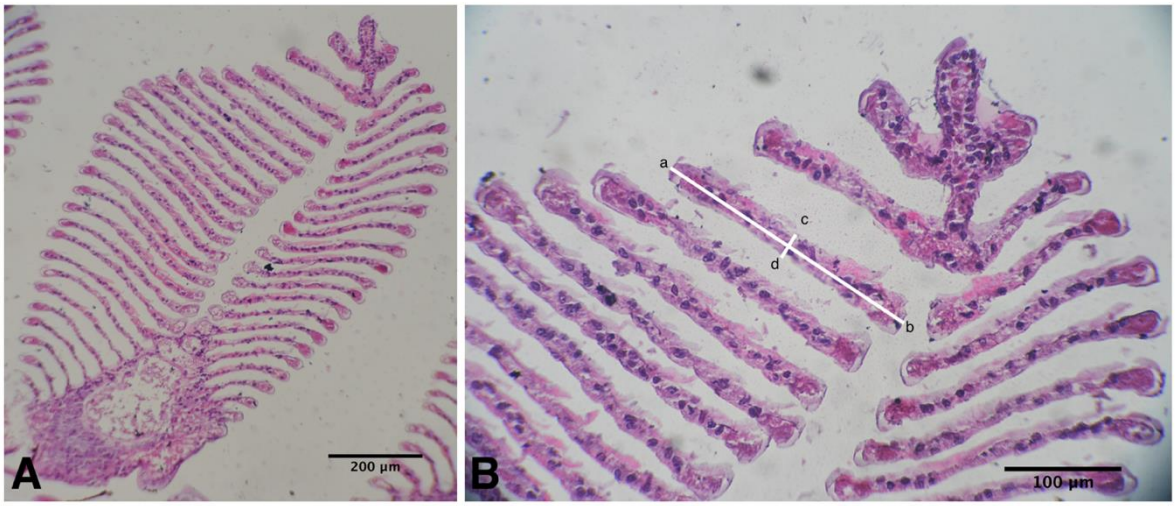

Figure S2: Histological images of gill from *P. varians*. **A)** Micrograph showing the entire gill (20x magnification). **B)** Detail of the gill (40x magnification). From the section of each lamellae, the "best fitting ellipse" function from ImageJ returned the major axis (lamellar length – ab) and minor axis (lamellar width – cd) of the best fitting ellipse. Major and minor axis were then used to calculate lamellar perimeter.

378

Assembly Report with Scaffolded regions		
Total reads		95,513,752
Generated contigs		105,325
Minimum length		250 bp
Average length		907 bp
Median length		1491 bp
Maximum length		26718 bp
Mapping Report		
Mapped reads		82.29%
Not mapped reads		17.71%
Read in pairs		75.02%
RNA-seq Experiment Report		
Reference Transcriptome (n° contigs)		59,370
	Normoxia	Hypoxia
Mapping reads	68.64%	75.05%
Uniquely mapping reads	68.43%	74.82%
Not-uniquely mapping reads	0.21%	0.23%

379

380 Table S3: Transcriptome statistics

381

382

383

Upregulated

Description:	Contig ID	Proportional fold change:	UniprotKB accession number	GenBank
Chitinase 2	contig_13969	235.39	Q9W5U2	BAA14014.1
Post-moult protein 1	contig_16319	189.1	A0A0K2C0S2	AKZ75936.1
Cuticle protein	contig_54328	138.18	P81388	
Cuticle protein	contig_66705	58.45	P81388	
Chemosensory protein 3	contig_38778	36.64		ABH88168.1
Elongation of very long chain fatty acids protein	contig_47915	26.8	Q1HRV8	
Cuticle protein	contig_25634	20.73	P81576	
Cuticle protein	contig_60605	20.54	P81576	
Cuticle protein	contig_34320	16.45	P81577	
Cuticle protein	contig_58327	15.86	P81388	
Chemosensory protein 3	contig_62563	15.78		ABH88168.1
Cuticle protein	contig_35509	13	P81589	
RNA-binding protein like	contig_16807	12.71	Q5RBM8	
Chitinase	contig_25080	11.97	Q9W5U2	
Peptide M28	contig_20072	11.45	A0A0R6QQU2	
Cuticle protein	contig_5295	8.64	P81580	
Cuticle protein	contig_8285	8.46	P82119	
Cuticle protein	contig_719	8.42	P81589	
Cuticle protein	contig_14361	8.18	P81582	
Cuticle protein	contig_3086	8.1	P82119	
Cuticle protein	contig_54327	7.71	P81579	
Retinoid-inducible serine carboxypeptidase	contig_16170	7.49	Q9HB40	
Cuticle protein	contig_35105	7.32	P81579	
Gastrolith protein 18	contig_7251	7.28		ALC79580.1
Cuticle protein	contig_8790	7.15	P81585	
Cuticle protein	contig_7102	6.98	P81580	
Cuticle protein	contig_14360	6.94	P81582	
Cuticle protein	contig_8789	6.86	P81580	
Post-moult protein 1	contig_16101	6.84		AKZ75936.1
Cuticle protein	contig_747	6.56	P81580	
Cuticle protein	contig_7970	6.52	P81388	
Cuticle protein	contig_60747	6.48	P81584	
Cuticle protein	contig_8284	6.34		
Post-moult protein 1	contig_16100	6.22		AKZ75936.1
Cuticle protein	contig_795	6.2	P82119	
Post-moult protein 1	contig_16102	6.16		AKZ75936.1
Gastrolith protein 18	contig_11672	6.15		ALC79580.1
Cuticle protein	contig_718	5.95	P81589	
Glucose-6-phosphate transporter	contig_12820	5.9	O43826	
Cuticle protein	contig_6370	5.49	P81589	
Calcification associated peptide	contig_10413	5.31		BAD16776.1
Cuticle protein	contig_4477	4.96	P81583	
Larval cuticle protein	contig_5276	4.93		JAG02058.1
Cuticle protein	contig_107	4.92	P82119	
Gastrolith protein 30	contig_33893	4.9	O76217	
DD5 peptide	contig_23547	4.72	Q7M4F4	
Alkaline phosphatase	contig_791	4.51	Q92058	

Down-regulated

Description:	Contig ID	Proportional fold change:	UniprotKB accession number	GenBank
Vitellogenin	contig_15601	-31.37	Q6RG02	
Alpha-2 macroglobulin	contig_1092	-7.09		AEC50080.1
Peritrophin C	contig_2074	-6.12		ADE06398.1
Hemocyanin B chain	contig_1471	-5.69	P10787	
Serpin serine protease inhibitor	contig_7339	-5.26	Q8VHP7	
Insulin-like androgenic gland factor	contig_7365	-4.48		BAJ84108.1
Serine–threonine kinase	contig_5351	-4.3	Q9QYZ3	
Endochitinase	contig_3019	-3.92	P36362	
Cuticular protein analogous to peritrophins	contig_752	-3.87		JAN84453.1
Chitinase	contig_25081	-3.47	Q9W5U2	
Vigilin	contig_4806	-3.35	Q8VDJ3	
Serine–threonine kinase	contig_5352	-3.17	Q9QYZ3	
Chitinase	contig_8095	-2.96	H2A0L4	
Serine–threonine kinase	contig_1214	-2.92	Q9QYZ3	
Serine–threonine kinase	contig_7112	-2.89	P38692	
Serine–threonine kinase	contig_3557	-2.85	Q8VCT9	
Vigilin	contig_13004	-2.84	Q00341	
Fibrillin 2	contig_7351	-2.83	Q14246	
Serine–threonine kinase	contig_598	-2.81	Q54XJ4	
TATA box-binding protein-like 1	contig_271	-2.78	Q9YGV8	
Antimicrobial peptide (Crustin 7)	contig_466	-2.67		AOF80302.1
Serine–threonine kinase	contig_9498	-2.57	Q54PX0	
EGF-like module-containing mucin-like hormone receptor-like 1	contig_13978	-2.53	Q14246	
Hemocytin	contig_1311	-2.46		XP_020279864.1
EGF-like module-containing mucin-like hormone receptor-like 1	contig_7350	-2.45	Q14246	
Protein-tyrosine kinase	contig_597	-2.42	Q9YHZ5	
Pim 1	contig_5174	-2.42	Q924U5	
Innexin	contig_17765	-2.39	O61787	
Acyl-CoA:lysophosphatidylglycerol acyltransferase 1	contig_2915	-2.34	Q91YX5	
Chitinase	contig_3729	-2.29	Q9W5U3	
TPA zinc finger protein	contig_2262	-2.28	P10394	
Proto-oncogene tyrosine-protein kinase ROS	contig_3558	-2.26	P11799	
Protein-tyrosine kinase	contig_2031	-2.22	Q9RRH3	
Chitinase	contig_1734	-2.2	Q9W5U4	

Table S4: List of putative responsive genes statistically up/down regulated in comparison to controls. Differential expression between treatment and control was calculated using a Kal's Z-test on proportions with FDR <0.05 and proportional fold change > |2|.

UP-REGULATED

eggNOG

Category:	Description:	p-value:
COG1819	Glycosyltransferase	4.03E-006

GO molecular function

Category:	Description:	p-value:
GO:0042302	Structural constituent of cuticle	3.33E-016
GO:0008061	Chitin binding	3.35E-003

InterPro

Category:	Description:	p-value:
IPR031311	Chitin-binding type R&R consensus	3.77E-015
IPR029277	Single domain Von Willebrand factor type C domain	3.98E-010
IPR012539	Crustacean cuticle	2.11E-015
IPR002557	Chitin binding domain	5.19E-010
IPR002213	UDP-glucuronosyl/UDP-glucosyltransferase	1.03E-004
IPR000618	Insect cuticle protein	4.56E-014

PFAM

Category:	Description:	p-value:
PF00379.20	Insect cuticle protein	5.95E-012
PF15430.3	Single domain von Willebrand factor type C	1.79E-009
PF00201.15	UDP-glucuronosyltransferase	1.29E-003
PF01607.21	carbohydrate-binding module (CBM)	2.79E-010
PF08140.8	Crustacean cuticle protein repeat	2.30E-013

DOWN-REGULATED

eggNOG

Category:	Description:	p-value:
COG3325	Chitinase	9.75E-005
COG0515	Serine Threonine protein kinase	2.82E-006

GO cellular components

Category:	Description:	p-value:
GO:0009897	External side of plasma membrane	1.52E-004

GO biological processes

Category:	Description:	p-value:
GO:0000272	Polysaccharide catabolic process	2.43E-007
GO:0007218	Neuropeptide signaling pathway	1.25E-003
GO:0007186	G-protein coupled receptor signaling pathway	2.30E-003
GO:0008203	Cholesterol metabolic process	5.02E-004
GO:0006032	Chitin catabolic process	2.86E-007

GO molecular function

Category:	Description:	p-value:
GO:0004867	Serine-type endopeptidase inhibitor activity	2.98E-003
GO:0004568	Chitinase activity	5.97E-007
GO:0008061	Chitin binding	2.53E-006
GO:0004672	Protein kinase activity	4.11E-003
GO:0004674	Protein serine/threonine kinase activity	4.10E-007
GO:0005524	ATP binding	1.48E-003

InterPro

Category:	Description:	p-value:
IPR011009	Protein kinase-like domain	2.01E-012
IPR004087	K Homology domain	1.24E-004
IPR004088	K Homology domain, type 1	7.31E-006
IPR001881	EGF-like calcium-binding domain	3.18E-003
IPR017441	Protein kinase, ATP binding site	4.55E-007
IPR013781	Glycoside hydrolase, catalytic domain	5.76E-003
IPR000719	Protein kinase domain	2.93E-011
IPR008271	Serine/threonine-protein kinase, active site	1.56E-008
IPR021109	Aspartic peptidase domain	1.51E-005
IPR013026	Tetratricopeptide repeat-containing domain	5.76E-003
IPR011990	Tetratricopeptide-like helical domain	5.95E-005
IPR002290	Serine/threonine/dual specificity protein kinase	7.31E-004
IPR018097	EGF-like calcium-binding, conserved site	1.89E-003
IPR001223	Glycoside hydrolase family 18, catalytic domain	7.15E-004
IPR002557	Chitin binding domain	1.09E-003
IPR014756	Immunoglobulin E-set	5.23E-003
IPR000152	EGF-type aspartate/asparagine hydroxylation site	1.89E-003

PFAM

Category:	Description:	p-value:
PF07645.12	Calcium-binding epidermial growth factor domain	1.34E-003
PF00013.26	K Homology (KH) domain	1.60E-006
PF07719.14	Tetratricopeptide repeat	6.06E-005
PF00704.25	Glycoside hydrolase family 18 (probably Chitinase II)	5.41E-003
PF13975.3	gag-polyprotein putative aspartyl protease	7.10E-007
PF00069.22	Protein kinase domain	1.97E-007

Table S5: Hypergeometric tests on categories, performed on each of the annotation categories of the sub-set of differentially expressed genes with the following criteria: p- value <0.01 and “Observed – Expected Difference” ≥3.

References:

Benson, B. B., & Krause, D. (1984). The concentration and isotopic fractionation of oxygen dissolved in freshwater and seawater in equilibrium with the atmosphere. *Limnology and Oceanography, 29*(3), 620-632.

Bouchon, D. (1991a). Biological clock in seasonal reproductive cycle in the ditch shrimp *Palaemonetes varians* (Leach). II. Ovarian state-dependent response to non-diel light-dark cycles. *Journal of Experimental Marine Biology and Ecology, 146*(1), 13-26. doi:10.1016/0022-0981(91)90252-R

Bouchon, D. (1991b). Biological clock in seasonal reproductive cycle in the ditch shrimp *Palaemonetes varians* Leach. I. Photoperiodic time measurement. *Journal of Experimental Marine Biology and Ecology, 146*(1), 1-12. doi:10.1016/0022-0981(91)90251-Q

Brouwer, M., Brown-Peterson, N. J., Larkin, P., Patel, V., Denslow, N., Manning, S., & Brouwer, T. H. (2007). Molecular and whole animal responses of grass shrimp, *Palaemonetes pugio*, exposed to chronic hypoxia. *Journal of Experimental Marine Biology and Ecology, 341*(1), 16-31. doi:10.1016/j.jembe.2006.10.049

Burnham, K. P., Anderson, D. R., & Huyvaert, K. P. (2011). AIC model selection and multimodel inference in behavioral ecology: some background, observations, and comparisons. *Behavioral Ecology and Sociobiology, 65*(1), 23-35. doi:10.1007/s00265-010-1029-6

Bustin, S. A. (2010). Why the need for qPCR publication guidelines?--The case for MIQE. *Methods, 50*(4), 217-226. doi:10.1016/j.ymeth.2009.12.006

Carniel, F. C., Gerdol, M., Montagner, A., Banchi, E., De Moro, G., Manfrin, C., . . . Tretiach, M. (2016). New features of desiccation tolerance in the lichen photobiont *Trebouxia gelatinosa* are revealed by a transcriptomic approach. *Plant Molecular Biology, 91*(3), 319-339. doi:10.1007/s11103-016-0468-5

Ern, R., Huong, D. T. T., Nguyen, V. C., Wang, T., & Bayley, M. (2013). Effects of salinity on standard metabolic rate and critical oxygen tension in the giant freshwater prawn (*Macrobrachium rosenbergii*). *Aquaculture Research, 44*(8), 1259-1265.

Falcon, S., & Gentleman, R. (2007). Using GOstats to test gene lists for GO term association. *Bioinformatics, 23*(2), 257-258. doi:10.1093/bioinformatics/btl567

Fass, S., Ganaye, V., Urbain, V., Manem, J., & Block, J. C. (1994). Volatile fatty-acids as organic-carbon sources in denitrification. *Environmental Technology, 15*(5), 459-467.

Grabherr, M. G., Haas, B. J., Yassour, M., Levin, J. Z., Thompson, D. A., Amit, I., . . . Regev, A. (2011). Full-length transcriptome assembly from RNA-Seq data without a reference genome. *Nature Biotechnology, 29*(7), 644-U130. doi:10.1038/nbt.1883

Herreid, C. F. (1980). Hypoxia in invertebrates. *Comparative Biochemistry and Physiology Part A: Physiology, 67*(3), 311-320. doi:10.1016/S0300-9629(80)80002-8

Ikeya, T., Persson, P., Kono, M., & Watanabe, T. (2001). The DD5 gene of the decapod crustacean *Penaeus japonicus* encodes a putative exoskeletal protein with a novel tandem repeat structure. *Comparative Biochemistry and Physiology Part B: Biochemistry and Molecular Biology, 128*(3), 379-388. doi:10.1016/S1096-4959(00)00335-3

Inoue, H., Ohira, T., Ozaki, N., & Nagasawa, H. (2004). A novel calcium-binding peptide from the cuticle of the crayfish, *Procambarus clarkii*. *Biochemical and Biophysical Research Communications, 318*(3), 649-654. doi:10.1016/j.bbrc.2004.04.075

Kal, A. J., van Zonneveld, A. J., Benes, V., van den Berg, M., Koerkamp, M. G., Albermann, K., . . . Tabak, H. F. (1999). Dynamics of gene expression revealed by comparison of serial analysis of gene expression transcript profiles from yeast grown on two different carbon sources. *Molecular biology of the cell, 10*(6), 1859-1872.

Marshall, D. J., Bode, M., & White, C. R. (2013). Estimating physiological tolerances - a comparison of traditional approaches to nonlinear regression techniques. *Journal of Experimental Biology, 216*(Pt 12), 2176-2182. doi:10.1242/jeb.085712

Mueller, C. A., & Seymour, R. S. (2011). The regulation index: a new method for assessing the relationship between oxygen consumption and environmental oxygen. *Physiological and Biochemical Zoology, 84*(5), 522-532. doi:10.1086/661953

Oliphant, A. (2013). *Decapod crustacean larval developmental plasticity and the evolution of lecithotrophy and abbreviated development.* University of Southampton.

Oliphant, A., & Thatje, S. (2014). Energetic adaptations to larval export within the brackish-water palaemonine shrimp, *Palaemonetes varians*. *Marine Ecology Progress Series, 505*, 177-191. doi:10.3354/meps10767

Oliphant, A., Thatje, S., Brown, A., Morini, M., Ravaux, J., & Shillito, B. (2011). Pressure tolerance of the shallow-water caridean shrimp *Palaemonetes varians* across its thermal tolerance window. *Journal of Experimental Biology, 214*(Pt 7), 1109-1117. doi:10.1242/jeb.048058

Qing, G., Kikuchi, R., Kishira, S., Takagaki, A., Sugawara, T., & Oyama, S. T. (2016). Ammonia synthesis by N2 and steam electrolysis in solid-state cells at 220° C and atmospheric pressure. *Journal of The Electrochemical Society, 163*(10), E282-E287.

Quevillon, E., Silventoinen, V., Pillai, S., Harte, N., Mulder, N., Apweiler, R., & Lopez, R. (2005). InterProScan: protein domains identifier. *Nucleic Acids Research, 33*(Web Server issue), W116-120. doi:10.1093/nar/gki442

Roer, R., Abehsera, S., & Sagi, A. (2015). Exoskeletons across the Pancrustacea: comparative morphology, physiology, biochemistry and genetics. *Integrative and Comparative Biology, 55*(5), 771-791. doi:10.1093/icb/icv080

Sakamoto, Y., Ishiguro, M., & Kitagawa, G. (1986). Akaike information criterion statistics. *Dordrecht, The Netherlands: D. Reidel*.

Schneider, C. A., Rasband, W. S., & Eliceiri, K. W. (2012). NIH Image to ImageJ: 25 years of image analysis. *Nature Methods, 9*, 671-675. doi:10.1038/nmeth.2089

Simao, F. A., Waterhouse, R. M., Ioannidis, P., Kriventseva, E. V., & Zdobnov, E. M. (2015). BUSCO: assessing genome assembly and annotation completeness with single-copy orthologs. *Bioinformatics, 31*(19), 3210-3212. doi:10.1093/bioinformatics/btv351

Sun, S. M., Xuan, F. J., Fu, H. T., Zhu, J., Ge, X. P., & Gu, Z. M. (2015). Transciptomic and histological analysis of hepatopancreas, muscle and gill tissues of oriental river prawn (*Macrobrachium nipponense*) in response to chronic hypoxia. *BMC Genomics, 16*, 13. doi:10.1186/s12864-015-1701-3

Team, R. C. (2014). R: A language and environment for statistical computing. R Foundation for Statistical Computing, Vienna, Austria. URL http://www.r-project.org/.

Wood. (2006). *Generalized additive models: an introduction with R*: CRC press.